

# CHIMERA: A Hybrid Estimation Approach to Limit the Effects of False Data Injection Attacks

Xiaorui Liu<sup>\*†</sup>, Yaodan Hu<sup>†‡</sup>, Charalambos Konstantinou<sup>\*</sup>, Yier Jin<sup>†</sup>

<sup>\*</sup>FAMU-FSU College of Engineering, Center for Advanced Power Systems, Florida State University

<sup>†</sup>Department of Electrical and Computer Engineering, University of Florida

E-mail: xliu9@fsu.edu, cindy.hu@ufl.edu, ckonstantinou@fsu.edu, yier.jin@ece.ufl.edu

**Abstract**—The reliable operation of the electric power systems is supported by energy management systems (EMS) that provide monitoring and control functionalities. Contingency analysis is a critical application of EMS to evaluate the impacts of outage events based on the grid state variables, and allow system operators to prepare for potential system failures. However, false data injection attacks (FDIAs) against state estimation have demonstrated the possibility of compromising sensor measurements and consequently falsifying the estimated power system states. As a result, FDIAs may mislead the system operations and other EMS applications including contingency analysis and optimal power flow routines. In this paper, we assess the effect of FDIAs on contingency analysis and demonstrate that such attacks can affect the resulted number of contingencies in power systems. In order to mitigate the FDIA impact on contingency analysis algorithms, we propose CHIMERA, a hybrid attack-resilient state estimation approach that integrates model-based and data-driven methods. CHIMERA combines the physical grid information with a Long Short Term Memory (LSTM)-based deep learning model by considering a static loss of weighted least square errors and a dynamic loss of the difference between the temporal variations of the actual and the estimated active power. Our simulation experiments based on the load data from New York state demonstrate that CHIMERA can effectively mitigate 91.74% of the attack cases in which FDIAs can maliciously modify the contingency results.

**Index Terms**—Electric power grid, false data injection attacks, contingency analysis, hybrid state estimation.

## I. INTRODUCTION

In electric power grids, energy management systems (EMS) provide situational awareness and assist the decision-making for system operators. EMS encompasses hardware/field components at geographically dispersed locations, e.g., remote terminal units (RTUs) and telecommunications systems, as well as software applications at utility control centers, e.g., state estimation and contingency analysis. Specifically, the network topology processor within EMS utilizes breaker status and acquired data from RTUs and telemetry devices to update the power system model. The collected measurements and the updated system model facilitate the state estimator to determine the current system states. The estimated results are required by other EMS applications such as contingency analysis and optimal load flow algorithms. Thus, the accuracy of EMS applications depends on the results of state estimation.

As part of state estimation routines, bad data detection (BDD) units are used to identify anomalous measurements and enhance the security and accuracy of the estimation. However, it has been shown that attackers could launch false data injection attacks (FDIAs) and bypass BDD by injecting malicious data into the collected measurements required for state estimation [1]. Undetectable FDIAs under the situation of sensor failures could even worsen the estimation performance [2]. In addition, the conditions of the 2015 attack on the Ukrainian power grid, demonstrated that the threat model of FDIAs is sufficient to result in massive blackouts [3], [4].

Contingency analysis is one of the core applications in EMS used to predict system conditions under specific outage scenarios. It simulates and evaluates the impact of the planned or unplanned problems that occur in the electric grid such as scheduled maintenance and component failures. Components refer to generators, transmission lines, transformers, circuit breakers, etc. According to the North American Electric Reliability Corporation (NERC), the fundamental criterion of  $N-1$  (where  $N$  refers to the total number of components) requires that the power system is able to withstand the disruption of one component outage [5]. Contingency scenarios can be extended to  $N-k$ , which refers to a number of  $k$  component failures in the system. Grid operators rely on contingency analysis to recognize system overload conditions and rank the severity of the overloaded components by comparing the calculated results with the threshold of operation limits such as power flow constraints and thermal constraints of transmission lines. If such limits are exceeded after a contingency event, operators could isolate the overloaded components to prevent cascading failures. However, the reliability of contingency algorithms cannot be guaranteed when the system is under FDIAs. Such attacks cannot only affect state estimation, but also falsify the outcomes of contingency analysis [6].

To detect the FDIAs in power grids, two major detection approaches are considered in literature [7], model-based and data-driven methods. Model-based methods leverage the physics and data of the system (e.g., the grid topology and lines admittance) to estimate system states with methods such as recursive weighted least square and Kalman filters [8], [9]. In order to determine whether or not an attack occurs, different tests are applied to the estimation results such as the large normalized residual [10], [11], and the cumulative sum test [9]. Although the existing research on model-based

<sup>†</sup>The first two authors contributed equally to this work.

This work is supported in part by Cyber Florida under Collaborative Seed Award #3910-1011-00-A.

techniques aiming to develop BDD methods resilient against FDIAs, such methods are typically computationally expensive in terms of processing time and scalability [12]. For example, the authors in [13] deploy distributed flexible AC transmission system devices and activate them stochastically to enhance system hardening against attacks. The reconfiguration of system settings and topology would require recalculation of the power flow. Other works focus on data-driven methods to dynamically detect FDIAs, such as deep learning-based schemes [14], [15]. Despite the benefits of data-based approaches in terms of short execution times [16], such techniques require a large set of training data to achieve good performance. In the scenarios of network topology reconfigurations, such methods require retraining to ensure that learning models stay accurate. In addition, the rise of learning-based schemes in many applications is accompanied with important security challenges: it creates an incentive among adversaries to exploit potential vulnerabilities of the algorithms [17]–[19]. For instance, it is demonstrated solely artificial neural network-based estimation algorithms can be maliciously compromised [20].

Recent works illustrated that combining the physics-based models with data-based approaches provides several advantages, and specifically in terms of security, it tightly confines the solution scope and limits the capability of the adversarial examples [21]–[23]. For example, in order to have robust state estimation results, the authors in [22] introduce a physics-guided deep learning model for time-series power system state estimation which uses the sequential measurements as inputs to reduce the high dependency of the current measurements. Moreover, a hybrid method is utilized in [23] to enhance the reliability of the state estimation results, where the data-driven estimator is combined with a topology identification method to track system states and the model-based estimator is used for filtering the noises and gross errors from the measurements.

In this paper, we study the impacts of FDIAs on state estimation and contingency analysis, and propose a hybrid, model-based and data-driven, attack-resilient state estimator to mitigate the attack impact on the contingency analysis results. To the best of our knowledge, this paper is the first study to propose a hybrid estimation approach on how to mitigate the effect of FDIAs on contingency analysis. Our contributions are summarized as follows:

- We formulate an attack model in which the attacker is able to bypass state estimation BDD routines and cause, via FDIAs, non-critical power grid transmission lines, i.e., lines not included in the contingency screening, to surpass their power flow limits. We show that the impact of FDIAs can effectively distort the number of system contingencies.
- In order to mitigate the attack impact, we propose CHIMERA, a hybrid attack-resilient state estimator. i.e., a physics-informed estimator constructed based on Long Short Term Memory (LSTM) networks. It embeds the grid observation model of power flow equations into neural networks to enhance grid resilience against FDIAs. We exploit the static and dynamic features of the observation model to construct spatial-temporal correlations among mea-

surements, and limit how FDIAs against state estimation can affect subsequent EMS contingency results.

- We conduct simulation experiments based on load data from New York state. The results demonstrate that CHIMERA can effectively mitigate 91.74% of the attack cases in which FDIAs can maliciously modify the contingency results.

The rest of this paper is as follows: Section II provides background information. Section III discusses our attack model, and Section IV demonstrates the mitigation strategy against FDIAs. Experiments are presented in Section V, and Section VI draws concluding remarks.

## II. BACKGROUND

### A. State estimation

In the nonlinear (AC) state estimation of power systems, state variables are determined by phase angles ( $\theta$ ) and voltage magnitudes ( $V$ ). For a system with  $n$  buses, the state variables  $\mathbf{x}$  can be written as  $\mathbf{x} = [\theta_2, \theta_3, \dots, \theta_n, V_1, \dots, V_n]^T$ , where  $\theta_1 = 0$  is the reference angle. To maintain full observability of the system,  $m \geq n$  measurements are required. Measurements ( $\mathbf{z}$ ) typically include active power ( $P$ ) and reactive power ( $Q$ ) measurements. The relationship between states and acquired measurements, with  $\mathbf{e}$  being a vector of noises, is as follows:

$$\mathbf{z} = \mathbf{h}(\mathbf{x}) + \mathbf{e} \quad (1)$$

State estimation is widely solved via iterative techniques such as the weighted least square method [24], in which the accuracy of the estimated variables  $\hat{\mathbf{x}}$  is calculated via the Euclidean norm of the residual  $\|\mathbf{z} - \mathbf{h}(\hat{\mathbf{x}})\|$ . For example, the estimated states  $\hat{\mathbf{x}}$  can be obtained through optimization of  $J(\hat{\mathbf{x}})$  in Eq. (2), where  $\mathbf{W} = \text{diag}\{\sigma_1^{-2}, \sigma_2^{-2}, \dots, \sigma_m^{-2}\}$  composes all the weights  $\sigma^{-2}$  of the measurements. There are different approaches to solve Eq. (2); one such method is via iteratively solving Eq. (3). To detect whether or not the state estimation is disturbed by the random noises or attacks, BDD compares the objective function  $J(\hat{\mathbf{x}})$  with a normalized threshold  $\tau$ . If  $J(\hat{\mathbf{x}}) < \tau$ , no bad data is detected.

$$\min_{\hat{\mathbf{x}}} J(\hat{\mathbf{x}}) = (\mathbf{z} - \mathbf{h}(\hat{\mathbf{x}}))^T \mathbf{W} (\mathbf{z} - \mathbf{h}(\hat{\mathbf{x}})) \quad (2)$$

$$\mathbf{H}_k^T \mathbf{W} \mathbf{H}_k \Delta \hat{\mathbf{x}}_k = \mathbf{H}_k^T \mathbf{W} [\mathbf{z} - \mathbf{h}(\hat{\mathbf{x}}_k)] \quad (3)$$

To reduce the computational overhead, linear (DC) state estimation is often adopted which makes several assumptions: the transmission line resistances are negligible, voltage magnitudes are 1 per unit, and the differences in voltage angles between buses are small. Thus, the observation model can be linearized:

$$P_i = \sum_{j \in N_i} \mathbf{B}_{ij} (\theta_i - \theta_j), \quad (4)$$

and in matrix form  $\mathbf{P} = \mathbf{H}\boldsymbol{\theta}$ , in which  $\mathbf{P}$  and  $\boldsymbol{\theta}$  are the vectors of the active power measurements and the voltage angles of the buses, respectively.  $\mathbf{H}$  is the measurement Jacobian matrix derived from the susceptance matrix  $\mathbf{B}$ . With the approximations, the accuracy of the estimation is decreased while the computation overhead is reduced. The states  $\boldsymbol{\theta}$  can be estimated with the following equation:

$$\tilde{\boldsymbol{\theta}} = (\mathbf{H}^T \mathbf{H})^{-1} \mathbf{H}^T \mathbf{P} \quad (5)$$

## B. Contingency Analysis

Contingency analysis simulates the effects of contingency/outage scenarios and calculates the overload conditions in the overall system. However, the computational cost of such “what-if” scenarios is unrealistic for large-scale and complex power systems. The computational overhead is proportional to  $N!/[k!(N - k)!]$  for  $N - k$  contingencies. Due to the low probability of  $N - 3$  contingencies occurring in different transmission lines in real-world [25], research works typically focus on  $N - 1$  and  $N - 2$  scenarios [26]. In order to find all power flow constraint violations under  $N - 1$  and  $N - 2$  scenarios, the linear power flow approximation is typically utilized [27]. Following such approach, in this work, the power flows are calculated by  $\mathbf{f} = \mathbf{Y}\mathbf{M}^T\boldsymbol{\theta}$ , where  $\mathbf{Y}$  is the branch susceptance matrix,  $\mathbf{M}$  is the connection matrix, and  $\boldsymbol{\theta}$  is the vector of voltage phase angles. Additionally,  $\mathbf{f}$  is used to calculate the line outage distribution factors (LODFs). LODFs determine the power flow impact on the remaining lines when one or more line outages are observed in the system. The mathematical formulation of single and double outages can be found in [28].

## III. ATTACK MODEL

### A. Threat Model

FDIAs have been traditionally demonstrated on how to compromise the state estimation process against system operations [7]. In this paper, we assume that the attacker does not solely target to falsify the state estimation but also to manipulate the contingency analysis results. We consider an attacker who can exploit the configuration of a power system to launch FDIAs by manipulating the sensor measurements while bypassing BDD. Moreover, the attacker targets those measurements to attack which could distort the number of contingencies. The assumptions of the threat model are as follow:

- The attacker has the full observation of the topology and configurations of the power system, i.e., the attackers could construct the Jacobian matrix  $\mathbf{H}$ . Such information can be obtained through public information or signal reconstruction [29], [30].
- The attacker is aware of the specifics of the state estimation process, either model-based or data-driven, in order to carefully craft FDIAs to bypass BDD routines.
- The attacker has access to the real-time measurements of deployed grid sensors, e.g., via eavesdropping on the communication links. However, due to the limited physical access or the protection of certain meters, the attacker can compromise a limited number of measurements [24].
- The attacker could perform contingency analysis based on the estimated results and the power flow constraints of each line required to ensure an overload condition [26].

### B. Mathematical Formulation

Despite BDD mechanisms can detect measurement anomalies, carefully crafted FDIAs can bypass such algorithms. Consider the malicious vector  $\mathbf{a}$  injected into measurements  $\mathbf{z}$ , then the compromised measurement vector can be represented

as  $\mathbf{z}_a = \mathbf{z} + \mathbf{a}$ . The resulted attacked estimated state variables can be written as  $\hat{\mathbf{x}}_a = \hat{\mathbf{x}} + \mathbf{c}$ , where  $\mathbf{c}$  is the vector of the injected and resulted error. A successful FDIA undetected by the residual-based BDD, as shown in Eq. (6), can be formed when  $\mathbf{a} = \mathbf{H}\mathbf{c}$ , i.e., if  $\mathbf{a}$  is a linear combination of  $\mathbf{H}$ , for the arbitrary vector  $\mathbf{c}$ .

$$\begin{aligned} \|r_a\| &= \|\mathbf{z}_a - \mathbf{H}(\hat{\mathbf{x}}_a)\| = \|\mathbf{z} + \mathbf{a} - \mathbf{H}(\hat{\mathbf{x}} + \mathbf{c})\| \\ &= \|\mathbf{z} + \mathbf{H}(\hat{\mathbf{x}} + \mathbf{c}) - \mathbf{H}(\hat{\mathbf{x}}) - \mathbf{H}(\hat{\mathbf{x}} + \mathbf{c})\| \\ &= \|\mathbf{z} - \mathbf{H}(\hat{\mathbf{x}})\| = \|r\| \end{aligned} \quad (6)$$

Fig. 1 depicts the overall process of the attack model. The sensor measurements  $\mathbf{z}$  are compromised by FDIAs represented by an attack vector  $\mathbf{a}$ . The estimated states  $\hat{\mathbf{x}}$ , as the output of the estimation process, will be altered under FDIAs. The BDD can detect and remove the significant errors as bad data, namely  $J(\hat{\mathbf{x}})$  above the threshold  $\tau$ . Otherwise, if BDD is bypassed due to FDIAs, the malicious states will be processed to perform contingency analysis. Since the power flow computation,  $\mathbf{f}^a$ , is affected, the contingency results  $\mathbf{f}^{a'}$  will be inaccurate. As a result, system operators will be misled by the malicious contingency analysis output, and thus, potential threats to the power system reliability may be posed.

Based on the assumptions of the attacker's capabilities and knowledge of the power system topology and data, the attack model is mathematically formulated as Eq. (7a) - (7g), where the attacker's objective is to affect the results of contingency analysis by FDIAs. In order to achieve that, the attacker performs contingency analysis to obtain the power flows under contingency and find the most vulnerable line  $i$  which has the smallest difference between its power flow under contingency  $f_i^{a'}$ , and its power flow capacity  $f_i^{limit}$ . The targeted line will overload based on the maximization function with an optimal attack vector  $\mathbf{a}$  through FDIAs, as shown in Eq.(7a). An absolute value of  $f_i^{a'}$  is used here to represent the overflow observed either with  $f_i^{a'} > f_i^{limit}$  or  $-f_i^{a'} > f_i^{limit}$ .

In order for the FDIAs to be stealthy and not being detected, several constraints represented by Eq. (7b) - (7g) should be satisfied. In practice, a safety margin  $f_m$  in the line flow capacity is reserved to reduce the overload risk. Therefore, only the line with a power flow below the certain line flow capacity  $f_i^{limit} - f_m$  will be considered, as described in (7b). Eq.(7c) shows that the attacker can compromise certain measurement  $\mathbf{z}$  to  $\mathbf{z}_a$  by adding an attack vector  $\mathbf{a}$ . Accordingly, the estimated state variables  $\hat{\mathbf{x}}$  will be deviated to  $\hat{\mathbf{x}}_a$  in (7d). In order to maintain stealth and bypass the BDD, the injected error should guarantee that the residual  $J(\hat{\mathbf{x}}_a)$  is within the system threshold  $\tau$ , as depicted in (7e). Once the malicious state variables are utilized to perform power flow computations, the results  $\mathbf{f}^a$  will be affected since the voltage phase angles  $\hat{\theta}_a$  in (7f) are part of the deviated estimated variables  $\hat{\mathbf{x}}$ . The factor  $\lambda^a$  to qualify the line overload condition, LODF, will be utilized to compute the power flows. Taking the compromised power flow equation at line  $i$  ( $f_i^a$ ), line  $j$  ( $f_j^a$ ) with the LODF, the power flow of line  $i$  under FDIAs with line  $j$  during a outage is derived as  $f_i^{a'}$  in (7g).

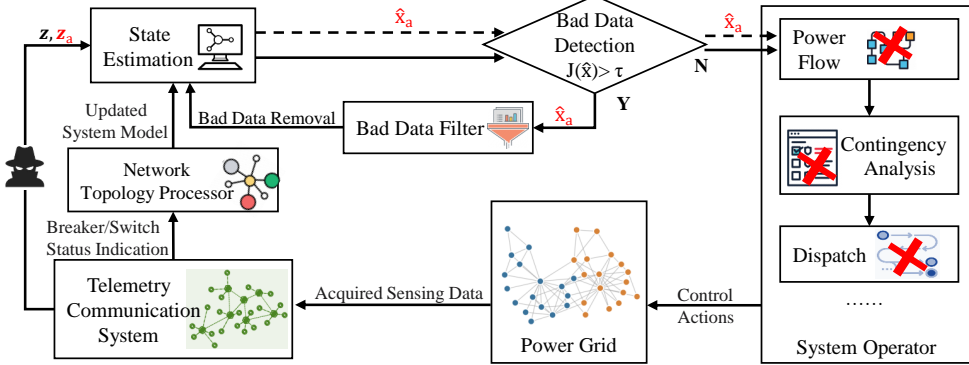


Fig. 1. Illustration of the attack model (attacked variables in red color).

$$\underset{\mathbf{a}}{\text{maximize}} \quad \underset{|f_i^{\mathbf{a}'}|}{\text{argmin}} \quad f_i^{\text{limit}} - |f_i^{\mathbf{a}'}| \quad (7a)$$

$$\text{subject to} \quad |f_i^{\mathbf{a}'}| < f_i^{\text{limit}} - f_m \quad (7b)$$

$$\mathbf{z}_a = \mathbf{z} + \mathbf{a} \quad (7c)$$

$$\hat{\mathbf{x}}_a = \hat{\mathbf{x}} + \mathbf{c} \quad (7d)$$

$$J(\hat{\mathbf{x}}_a) = (\mathbf{z} - \mathbf{h}(\hat{\mathbf{x}}_a))^T W (\mathbf{z} - \mathbf{h}(\hat{\mathbf{x}}_a)) < \tau \quad (7e)$$

$$\mathbf{f}^{\mathbf{a}} = \mathbf{Y} \mathbf{M}^T \hat{\boldsymbol{\theta}}_a \quad (7f)$$

$$f_i^{\mathbf{a}'} = \lambda_{ij}^{\mathbf{a}} f_j^{\mathbf{a}} + f_i^{\mathbf{a}} \quad (7g)$$

#### IV. CHIMERA: HYBRID ATTACK-RESILIENT STATE ESTIMATOR

In order to mitigate the impacts of FDIs on the state estimation and the consequential contingency analysis, we propose CHIMERA, a hybrid attack-resilient state estimator. CHIMERA is an AC state estimator, which takes active and reactive power measurements as well as DC-estimated voltage angles as the input, and provides estimates of voltage magnitudes and angles of the buses. Given the attack model presented in Section III and considering that a DC power flow model is typically used in grid operations [7], we build an AC hybrid estimator which is resilient to FDIs affecting EMS routines. Despite a corrupted DC estimation output  $\hat{\boldsymbol{\theta}}_t$ , CHIMERA provide accurate state predictions, by taking advantage of both the observation model Eq. (1) and an LSTM-based deep learning model. The LSTM network can capture the temporal correlations between data, and thus, the errors induced by the attacks can be corrected by the historical information. Moreover, since the observation model can confine the solution space with the physical constraints, we construct the loss function based on such a model.

In regards to the enhancement of the convergence speed and the estimation accuracy, we provide the DC estimation results  $\hat{\boldsymbol{\theta}}$  as the input of CHIMERA in addition to the power measurements ( $\mathbf{P}$ ,  $\mathbf{Q}$ ). Despite the limited accuracy of the DC estimation results due to the approximations, the DC estimated voltage angles can directly infer the scope of the true voltage angles. Thus, even in the presence of FDIs, we include

the DC estimated voltage angles in the input of CHIMERA because they can partially represent the states of the power grid. As a result, the input is formulated as  $\mathbf{u}_t = [\mathbf{z}_t; \hat{\boldsymbol{\theta}}_t]$ , in which  $\mathbf{z}_t$  and  $\hat{\boldsymbol{\theta}}_t$  are the vectors of the sensor measurements and the DC estimated states at time  $t$ , respectively.

To capture the spatio-temporal correlations of the observation model in the presence of benign and malicious data, the loss function of CHIMERA is composed of two parts: the static loss and the dynamic loss. In general, to regulate the accuracy of the estimated states, a typical way is to use the difference between the observed measurements and the derived measurements from the observation model Eq. (1) [17], [22], which is defined as the static loss:

$$L_{\text{static}} = \text{MSE}(\mathbf{z}_t, \mathbf{h}(\hat{\mathbf{x}}_t)), \quad (8)$$

in which  $\hat{\mathbf{x}}_t = [\hat{\boldsymbol{\theta}}_t; \hat{\mathbf{V}}_t]$  is the vector of estimated states from the model and consists of the vector of voltage angles  $\hat{\boldsymbol{\theta}}_t$  and magnitudes  $\hat{\mathbf{V}}_t$ .  $\text{MSE}(\mathbf{x}, \mathbf{y}) = (1/n) \sum_{i=1}^n (x_i - y_i)^2$  is the Mean Squared Error (MSE) between  $\mathbf{x}$  and  $\mathbf{y}$ . Nevertheless, with only  $L_{\text{static}}$ , the LSTM network cannot totally mitigate the impacts of FDIs, especially on contingency analysis. Although the structure of LSTM can utilize the temporal correlations of data implicitly, adversarial perturbations including FDIs on such recurrent neural networks have been proven effective [16]. Therefore, as also shown in Section V, depending solely on the temporal correlations from LSTM is insufficient to defend against the attack proposed in Section III. To better describe the temporal correlations between data, we further exploit the consistency of the observation model in the time domain and explicitly augment the loss function with the dynamic loss,  $L_{\text{dynamic}}$ . The dynamic loss measures the distance between the expected and the actual variations of the measurements. Given Eq. (4), we have:

$$\mathbf{P}_t - \mathbf{P}_{t-1} = \mathbf{H}(\hat{\boldsymbol{\theta}}_t - \hat{\boldsymbol{\theta}}_{t-1}), \quad (9)$$

in which  $\hat{\boldsymbol{\theta}}_t$  is the vector of the phase angles estimated by CHIMERA. Denote  $\Delta \mathbf{P}_t = \mathbf{P}_t - \mathbf{P}_{t-1}$  and  $\Delta \hat{\mathbf{P}}_t = \mathbf{H}(\hat{\boldsymbol{\theta}}_t - \hat{\boldsymbol{\theta}}_{t-1})$ . Thus the dynamic loss is defined as:

$$L_{\text{dynamic}} = \text{MSE}(\Delta \mathbf{P}_t, \Delta \hat{\mathbf{P}}_t). \quad (10)$$

The static loss,  $L_{static}$ , guarantees that the observation model is satisfied at each epoch, and the dynamic loss,  $L_{dynamic}$ , enforces the temporal consistency between the estimated states and the system measurements. Given  $L_{dynamic}$  and  $L_{static}$ , the loss function of CHIMERA is defined as:

$$L = L_{static} + \gamma L_{dynamic} \quad (11)$$

where  $\gamma \leq 1$  is the weight to balance the two terms. Compared with the loss function directly using the MSE between the estimated states and the true states, i.e.,  $L_0 = MSE(\hat{\mathbf{x}}, \mathbf{x})$  ( $\mathbf{x}$  is the vector of the true states), the proposed loss function  $L$  has several advantages. The true state  $\mathbf{x}$  is not required in  $L$ . Note that solving  $\mathbf{x}$  is non-trivial. The weighted least square method usually utilizes iterative methods to recursively minimize the residual  $J(\mathbf{x})$  in Eq. (2), which is often time-consuming, especially when the grid size increases. Therefore, the utilization of  $L_{static}$  and  $L_{dynamic}$  can boost timing performance while estimating the true system states. Besides, as mentioned in Section II-B, the accuracy of contingency analysis heavily relies on the accuracy of the estimated variables. Since  $L_{static}$  measures the difference between estimated and true power flows,  $L_{static}$  can enhance the accuracy of contingency results by enforcing the consistency between the estimated and true power flows. Unlike other FDIA defense methods, CHIMERA remains secure against other formulations of FDIA because the attack impact will be restrained as long as the accuracy of the estimation process is guaranteed.

The architecture of CHIMERA is depicted in Fig. 2. To avoid over-fitting, validation data is utilized to select the most suitable hyper-parameters for CHIMERA. We run CHIMERA with different configurations and select the one with the most accurate estimations on the validation data. The detailed configuration is explained as follows. CHIMERA is composed of two LSTM layers and a full connection layer. For each LSTM layer, the number of the features in the hidden state is 128 and the length of the sequence is 32. For the loss function, we set  $\gamma = 1 \times 10^{-3}$ . During the training phase, a batch of vectors  $\mathbf{u}_t$  with batch size 32 are provided as input. The outputs from the output layer  $\hat{\mathbf{x}}_t$  are then used to calculate the loss based on Eq. (11). The weights and the biases of the model are updated with the gradient of  $L$  by the Adam algorithm [31], through the back-propagation process. Due to the non-linearity of the observation model in Eq. (1), there are many local minimums. To approach the global minimum of  $L$ , we train the model with two steps. We first train a coarse model with a large learning rate  $1 \times 10^{-3}$  for 150 iterations. Then the model is fine-tuned for 500 iterations with small learning rates varying following a triangular cycle, which linearly increases from  $1 \times 10^{-7}$  to  $1 \times 10^{-4}$  and then decreases back to  $1 \times 10^{-7}$ .

## V. EVALUATION AND SIMULATION RESULTS

### A. Experimental Setup

1) *Dataset*: To examine the impacts of FDIA, we compare the number of contingencies and the overload conditions when the system is operated in normal conditions and under FDIA.

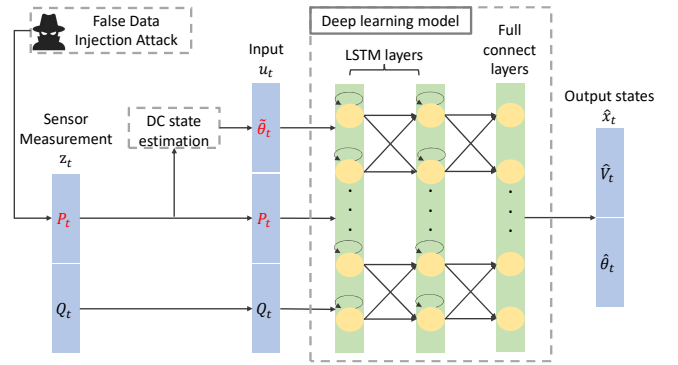


Fig. 2. The architecture of CHIMERA. The variables with red color are the ones that can be affected by FDIA.

Specifically, we conduct the experiment based on the IEEE 14-bus system and use synthetic data generated from the load data provided by the New York Independent System Operator (NYISO). We use NYISO load data from May 2020 containing the 5-min-interval active powers at each NY region, with 9030 epochs in total. The synthetic data is generated according to [21], and due to the unavailability of reactive power information, we generate the reactive power data by assuming a constant power factor of 0.8. White Gaussian noises with means of 0 and standard deviations of 0.01 are added to the measurements. We regard the measurements and the states generated as the ground truth when evaluating the performance of the estimation model. When executing contingency analysis, we use the flow limits listed in [32].

2) *Deep Learning Models for Evaluation*: In addition to CHIMERA, we train two models for comparison purposes: a Multilayer Perceptron (MLP) network and the model proposed in [22]. Since MLP induces limited computational overhead, it has been widely applied to the power grid [33]. In this paper, we train a MLP network as the performance baseline. The MLP is composed of three hidden layers with 128 neurons for the first two layers and 64 neurons for the last hidden layer. We use  $L_0 = MSE(\hat{\mathbf{x}}, \mathbf{x})$  as the loss function of MLP. Therefore, no additional information or system dynamics are leveraged to defend against FDIA. We refer to this model as the baseline MLP and use it to demonstrate the impacts of FDIA on the state estimation and the contingency analysis when no defense is considered. Besides the baseline MLP, we also utilize for comparison the physics-guided deep learning network proposed in [22], which encompasses a FDIA-resistant autoencoder based on LSTM and uses  $\mathbf{z}_t$  as the input and  $L_{static}$  as the loss function. We refer to this model as  $LSTM_{ref}$ .

The MLP and  $LSTM_{ref}$  are trained by following the same procedure as CHIMERA, i.e., 70% of the data is used for training, 15% for validation, and 15% for testing. The training times of the three models, deployed on a computing platform with an NVIDIA GTX 2048 and an eight-core Intel(R) Xeon(R) CPU of 2.60 GHz, are summarized in Table I. Because of the simple network architecture and loss

TABLE I  
TRAINING TIME OF THE BASELINE MLP,  $LSTM_{ref}$ , AND CHIMERA.

Model	Coarse train (s)	Fine tune (s)	Total time (s)
MLP	101.56	257.19	358.75
$LSTM_{ref}$	218.48	889.9	1108.38
CHIMERA	233.09	958.87	1191.96

function, the baseline MLP is trained faster than the other two models with a total time consumed for training to be 358.75s. CHIMERA makes a trade-off between training speed and security guarantees. It is trained slower than the other models, i.e., 1191.96s, because additional computations are conducted in the calculation of loss functions.

3) *Attack Setup*: We select the measurements to attack based on the criticalities of buses calculated according to [34]. The buses 1, 2, 3, 4, 5 have the highest criticalities. Thus the meters on those five buses are selected in order for the active power measurements to be injected with errors. The optimal attack vector of Eq. (7a) - (7g) is solved by the Adam algorithm with a learning rate of  $1 \times 10^{-2}$ . The attack vector is generated for the measurement vector at each epoch. We observe that more than 99% of the estimation result residuals from the three models are smaller than 0.5. Thus, the threshold of  $J(\hat{\mathbf{x}})$  is set as  $\tau = 0.5$  in the attack model. We run the attacks for different values of  $f_m$  and select  $f_m = 3$  based on the magnitudes of the injected errors. The injected errors have similar magnitudes for all three models. For each targeted measurement, the injected errors result in a Mean Absolute Error (MAE) of 0.55 for the baseline MLP, 0.54 for  $LSTM_{ref}$ , and 0.54 for CHIMERA.

#### B. Evaluation of the Estimation Results without Attacks

1) *Estimation Accuracy*: Denote the vectors of the true states and the estimated states at epoch  $t$  as  $\mathbf{x}_t = [\boldsymbol{\theta}_t; \mathbf{V}_t]$ , and  $\hat{\mathbf{x}}_t = [\hat{\boldsymbol{\theta}}_t; \hat{\mathbf{V}}_t]$ , respectively. Here  $\boldsymbol{\theta}_t$ ,  $\hat{\boldsymbol{\theta}}_t$ ,  $\mathbf{V}_t$  and  $\hat{\mathbf{V}}_t$  are the vectors of the true/estimated voltage angles and magnitudes, respectively. We use the Mean Absolute Percentage Error (MAPE):

$$MAPE(\mathbf{x}, \mathbf{y}) = \frac{1}{n} \sum_{i=1}^n \left| \frac{y_i - x_i}{x_i} \right|, \quad (12)$$

as the accuracy evaluation metric of the estimated states, and define  $MAPE_{\theta} = MAPE(\boldsymbol{\theta}_t, \hat{\boldsymbol{\theta}}_t)$ ,  $MAPE_V = MAPE(\mathbf{V}_t, \hat{\mathbf{V}}_t)$  and  $MAPE_{Total} = MAPE(\mathbf{x}_t, \hat{\mathbf{x}}_t)$ . The results are summarized in Fig. 3. Since the voltage angles fluctuate greater than the voltage magnitudes, the MSE of the angle estimations are larger than the MSE of the magnitude estimations. All three models achieve satisfiable accuracy with the average MAPEs of the states to be 1.02% for the baseline MLP, 1.70% for  $LSTM_{ref}$ , and 1.76% for CHIMERA.

2) *Contingency Analysis Results*: Given the estimated states from the three models, we perform contingency analysis to reveal the variance of the numbers of  $N - 1$  and  $N - 2$  contingencies in the system. By plugging the estimated states  $\hat{\mathbf{x}}_t$  into Eq. (1), we obtain the power flows  $\hat{\mathbf{f}}_t$ . The number

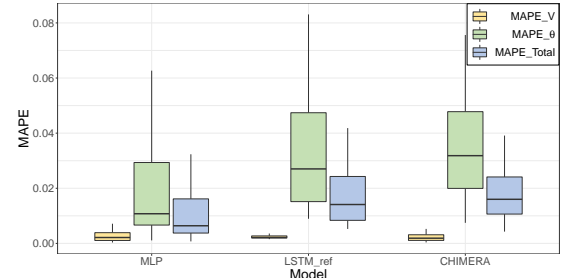


Fig. 3. MAPE of the estimated states from the baseline MLP,  $LSTM_{ref}$ , and CHIMERA in the attack-free scenario. In the attack-free scenario, MLP achieves the best accuracy in the voltage angle estimations and  $LSTM_{ref}$  achieves the best accuracy in the voltage amplitude estimations.

TABLE II  
AVERAGE PERFORMANCE OF THE THREE MODELS AGAINST FDIA.

Model	MAPE_V	MAPE_theta	MAPE_Total	$\epsilon_1^a$	$\epsilon_2^a$
MLP	0.27%	0.84%	0.54%	0.35	9.16
$LSTM_{ref}$	0.007%	0.12%	0.06%	0.03	5.75
CHIMERA	0.008%	0.14%	0.07%	0.06	1.70

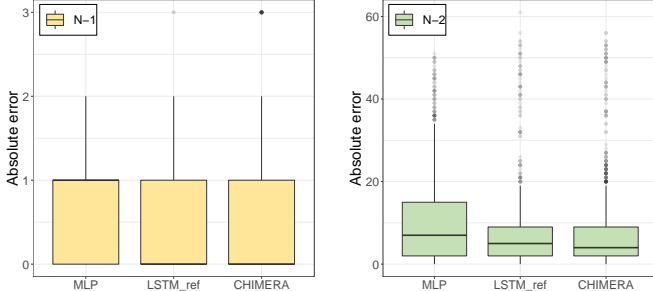
of the  $N - 1$  and the  $N - 2$  contingencies at epoch  $t$  given the estimated power flows  $\hat{\mathbf{f}}_t$  are denoted as  $\hat{N}_{1,t}$  and  $\hat{N}_{2,t}$ , respectively. Moreover, the contingency analysis based on the system measurements  $\mathbf{z}_t$  at each epoch  $t$  is executed to obtain the exact numbers of  $N - 1$  and  $N - 2$  contingencies in the system, which are denoted as  $N_{1,t}$  and  $N_{2,t}$ , respectively.  $N_{1,t}$  and  $N_{2,t}$  are referred to as the ground truth.

We use the absolute errors between the aforementioned methods of acquiring the contingency data, indicated with  $\epsilon_1 = |\hat{N}_{1,t} - N_{1,t}|$  and  $\epsilon_2 = |\hat{N}_{2,t} - N_{2,t}|$ , as the metric to evaluate the performance of the three models in the attack-free case. The results are shown in Fig. 4. Because of the estimation errors, errors are introduced into the contingency analysis results inevitably. The results demonstrate the benefit of  $L_{static}$  over  $L_0$ . Although the baseline MLP has the smallest MSE of state estimations,  $LSTM_{ref}$  and CHIMERA achieve better performance because  $L_{static}$  can enforce the consistency between the estimated power flows and the system measurements. For  $N - 1$  analysis, 68.60% and 69.12% of  $\hat{N}_{1,t}$  are accurately calculated ( $\epsilon_1 = 0$ ) for  $LSTM_{ref}$  and CHIMERA, respectively, while for the baseline MLP, only 46.50% of  $\hat{N}_{1,t}$  are accurately calculated. Besides, for  $N - 2$  analysis  $\hat{N}_{2,t}$ , the average  $\epsilon_2$  equals to 7.14 and 7.80 from  $LSTM_{ref}$  and CHIMERA, respectively, while the average  $\epsilon_2$  for  $\hat{N}_{2,t}$  from the baseline MLP is 10.30.

#### C. Impact of False Data Injection Attacks on Contingencies

The performance of the three models against FDIA is summarized in Table II. Overall,  $LSTM_{ref}$  and CHIMERA achieve better performance compared with the baseline MLP. Regarding the impacts of FDIA on the  $N - 2$  contingency analysis results, CHIMERA shows higher resilience to the attacks compared with  $LSTM_{ref}$ .

1) *Estimation Accuracy*: Denote the estimated states from attacked measurements as  $\hat{\mathbf{x}}_t^a$ . The impact of the attacks on



(a)

(b)

Fig. 4. The absolute errors of the numbers of (a)  $N - 1$  and (b)  $N - 2$  contingencies given the estimated power flows in the attack-free case. In the attack-free case,  $\text{LSTM}_{\text{ref}}$  and CHIMERA outperform MLP and achieve comparable performance in estimating the number of contingencies given the state estimates from the models.

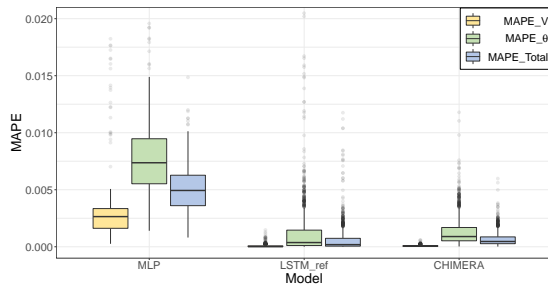
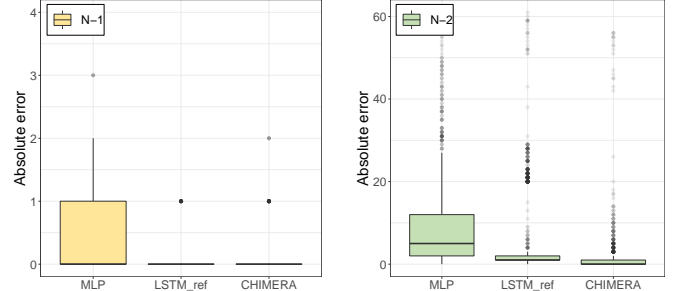


Fig. 5. The impact of the attacks on the estimation accuracy. In the occurrence of FDIAs,  $\text{LSTM}_{\text{ref}}$  and CHIMERA outperform MLP and achieve comparable performance regarding the state estimation accuracy.

the estimated states is assessed based on the  $MAPE_{\theta^a} = MAPE(\hat{\theta}_t, \hat{\theta}_t^a)$ ,  $MAPE_{V^a} = MAPE(\hat{V}_t, \hat{V}_t^a)$  and  $MAPE_{\text{Total}^a} = MAPE(\hat{x}_t, \hat{x}_t^a)$ . The results are summarized in Fig. 5. Note that the attacker intends to affect the contingencies while remaining undetected from the state estimation. The results verify the stealthiness of our attack model. We observe that the attacks do not induce large errors to the estimated states: the changes in the estimated states are only 0.54%, 0.06% and 0.07% for the baseline MLP,  $\text{LSTM}_{\text{ref}}$ , and CHIMERA, respectively. Despite the slight distinctions, we can still conclude that  $\text{LSTM}_{\text{ref}}$  and CHIMERA are more resilient to FDIAs due to their network architecture and the usage of  $L_{\text{static}}$ .

2) *Contingency Analysis Results:* Denote the number of the  $N - 1$  and the  $N - 2$  contingencies at epoch  $t$  given the power flows estimated from the attacked measurements as  $\hat{N}_{1,t}^a$  and  $\hat{N}_{2,t}^a$ . To assess the impacts of the attacks on the contingency analysis, we use the absolute errors between the number of contingencies from estimated power flows before and after attacks, i.e.,  $\epsilon_1^a = |\hat{N}_{1,t}^a - \hat{N}_{1,t}|$  and  $\epsilon_2^a = |\hat{N}_{2,t}^a - \hat{N}_{2,t}|$ , as the performance metrics. The results are presented in Fig. 6. If  $\epsilon_1^a$  or  $\epsilon_2^a$  are not equal to 0, an attack is considered successful. Besides, the larger  $\epsilon_1^a$  or  $\epsilon_2^a$  are, the larger the impact of the attack is. We observe that the contingency analysis results are sensitive to the accuracy of the estimated states. Although



(a)

(b)

Fig. 6. The impact of attacks on (a)  $N - 1$  and (b)  $N - 2$  contingency analysis. During occurrence of FDIAs,  $\text{LSTM}_{\text{ref}}$  and CHIMERA outperform MLP and achieve comparable performance regarding  $N - 1$  contingencies. CHIMERA outperforms  $\text{LSTM}_{\text{ref}}$  regarding  $N - 2$  contingencies.

the injected attack vectors have similar magnitudes and only slightly affect the accuracy of the estimated states, the impacts of the attacks on the contingency analysis results from the three models differ a lot. Since no defense is embedded in the baseline MLP, the performance of the baseline MLP is heavily degraded. In the  $N - 1$  case, 53.50% of  $\hat{N}_1^a$  are changed ( $\epsilon_1^a \neq 0$ ) for the baseline MLP, while the percentage of  $\hat{N}_1^a$  changed for  $\text{LSTM}_{\text{ref}}$  and CHIMERA are only 31.4% and 22.69%, respectively. The maximum  $\epsilon_1^a$  is 4 for the baseline MLP, while it is 1 and 2 for  $\text{LSTM}_{\text{ref}}$  and CHIMERA, respectively. In the  $N - 2$  case, the average  $\epsilon_2^a$  is 9.16 for the baseline MLP, while the average  $\epsilon_2^a$  is 5.75 for  $\text{LSTM}_{\text{ref}}$  and 1.70 for CHIMERA. Moreover, the results from  $\text{LSTM}_{\text{ref}}$  show that using only  $L_{\text{static}}$  cannot totally defend against FDIAs. On the other hand, because of the usage of the  $L_{\text{dynamic}}$ , the impact of FDIAs on CHIMERA is significantly limited. Specifically, 64.81% of attacks fail to take effect on CHIMERA, i.e.,  $\epsilon_2^a = 0$ , while the percentages for the baseline MLP and  $\text{LSTM}_{\text{ref}}$  are only 7.14% and 22.32%, respectively. Moreover, 91.74% of attacks have limited impacts on CHIMERA, i.e.,  $\epsilon_2^a < 5$ , while for the baseline MLP and  $\text{LSTM}_{\text{ref}}$  these values are 48.36% and 79.32%, respectively.

#### D. Practical Implications and Applications

In terms of real-world applications, CHIMERA can be implemented at the computing stations of power grid operators and be part of the EMS. For example, it can be deployed as an additional application in the EMS by updating the existing state estimation routines. Thus, CHIMERA does not require or induce any hardware modifications or overhead. The major computation cost of CHIMERA is on the training process. Despite that CHIMERA requires longer training time, since CHIMERA can be trained offline it does not induce additional computational overhead during runtime. In fact, the times for CHIMERA and MLP/ $\text{LSTM}_{\text{ref}}$  to estimate states are of the same order and approximately 0.05ms, which are neglectable and do not violate any real-time requirement operations of the EMS [35]. Furthermore, during attacks, significant enhancement has been achieved by CHIMERA in estimating the

number of  $N - 2$  contingencies. For the IEEE 14-bus system, there can be  $190 N - 2$  contingencies in total. Through our experiments, we show that in 91.74% attacks, CHIMERA can achieve an estimation accuracy more than 97.4% (i.e.,  $\epsilon_2^a < 5$ ) for  $N - 2$  contingencies. With such high accuracy, CHIMERA guarantees the normal operation of the power grid during the occurrence of FDIs.

## VI. CONCLUSIONS

In this paper, we investigate an attack model intending to disturb power systems contingencies through FDIs. We show that the attack can significantly manipulate contingency analysis accuracy by slightly increasing the state estimation errors. To mitigate the effects of such attacks, we propose CHIMERA, a hybrid attack-resilient state estimator which ensures the accuracy of state estimation and the resulting contingency analysis. CHIMERA leverages the dynamic and static features of the power grid observation model and embeds them into an LSTM-based deep learning model. Simulations are conducted on a power grid benchmark case with synthetic data generated from NYISO load data. The results justify the resilience of CHIMERA to FDIs and the capability of maintaining system operations in the EMS functions of state estimation and contingency analysis.

## REFERENCES

- [1] Y. Liu, P. Ning, and M. K. Reiter, “False data injection attacks against state estimation in electric power grids,” *ACM Transactions on Information and System Security (TISSEC)*, vol. 14, no. 1, pp. 1–33, 2011.
- [2] A.-Y. Lu and G.-H. Yang, “False data injection attacks against state estimation in the presence of sensor failures,” *Information Sciences*, vol. 508, pp. 92–104, 2020.
- [3] G. Liang *et al.*, “The 2015 ukraine blackout: Implications for false data injection attacks,” *IEEE Transactions on Power Systems*, vol. 32, no. 4, pp. 3317–3318, 2016.
- [4] I. Zografopoulos *et al.*, “Cyber-physical energy systems security: Threat modeling, risk assessment, resources, metrics, and case studies,” *IEEE Access*, vol. 9, pp. 29 775–29 818, 2021.
- [5] NERC, “Contingency Analysis - baseline,” <https://smartgrid.epri.com/UseCases/ContingencyAnalysis-Baseline.pdf>.
- [6] J.-W. Kang, I.-Y. Joo, and D.-H. Choi, “False data injection attacks on contingency analysis: Attack strategies and impact assessment,” *IEEE Access*, vol. 6, pp. 8841–8851, 2018.
- [7] A. S. Musleh, G. Chen, and Z. Y. Dong, “A survey on the detection algorithms for false data injection attacks in smart grids,” *IEEE Transactions on Smart Grid*, vol. 11, no. 3, pp. 2218–2234, 2019.
- [8] J. Sreenath *et al.*, “A recursive state estimation approach to mitigate false data injection attacks in power systems,” in *2017 IEEE Power & Energy Society General Meeting*. IEEE, 2017, pp. 1–5.
- [9] M. N. Kurt, Y. Yilmaz, and X. Wang, “Real-time detection of hybrid and stealthy cyber-attacks in smart grid,” *IEEE Transactions on Information Forensics and Security*, vol. 14, no. 2, pp. 498–513, 2018.
- [10] Z. Chu, “Unobservable false data injection attacks on power systems,” Ph.D. dissertation, Arizona State University, 2020.
- [11] H.-M. Chung *et al.*, “Local cyber-physical attack with leveraging detection in smart grid,” in *2017 IEEE International Conference on Smart Grid Communications (SmartGridComm)*. IEEE, 2017, pp. 461–466.
- [12] B. Li *et al.*, “Pama: A proactive approach to mitigate false data injection attacks in smart grids,” in *2018 IEEE Global Communications Conference (GLOBECOM)*. IEEE, 2018, pp. 1–6.
- [13] H. Salehghaffari and F. Khorrami, “Resilient power grid state estimation under false data injection attacks,” in *2018 IEEE Power & Energy Society Innovative Smart Grid Technologies Conference (ISGT)*. IEEE, 2018, pp. 1–5.
- [14] X. Niu, J. Li, J. Sun, and K. Tomovic, “Dynamic detection of false data injection attack in smart grid using deep learning,” in *2019 IEEE Power & Energy Society Innovative Smart Grid Technologies Conference (ISGT)*. IEEE, 2019, pp. 1–6.
- [15] Y. He, G. J. Mendis, and J. Wei, “Real-time detection of false data injection attacks in smart grid: A deep learning-based intelligent mechanism,” *IEEE Transactions on Smart Grid*, vol. 8, no. 5, pp. 2505–2516, 2017.
- [16] A. Sayghe *et al.*, “Survey of machine learning methods for detecting false data injection attacks in power systems,” *IET Smart Grid*, vol. 3, pp. 581–595, October 2020.
- [17] T. Liu and T. Shu, “Adversarial false data injection attack against nonlinear ac state estimation with ann in smart grid,” in *International Conference on Security and Privacy in Communication Systems*. Springer, 2019, pp. 365–379.
- [18] A. Sayghe, O. M. Anubi, and C. Konstantinou, “Adversarial examples on power systems state estimation,” in *2020 IEEE Power & Energy Society Innovative Smart Grid Technologies Conference (ISGT)*. IEEE, 2020, pp. 1–5.
- [19] A. Sayghe, J. Zhao, and C. Konstantinou, “Evasion attacks with adversarial deep learning against power system state estimation,” in *2020 IEEE Power & Energy Society General Meeting*. IEEE, 2020, pp. 1–5.
- [20] S. Aman, Y. Simmhan, and V. K. Prasanna, “Energy management systems: state of the art and emerging trends,” *IEEE Communications Magazine*, vol. 51, no. 1, pp. 114–119, 2013.
- [21] O. M. Anubi and C. Konstantinou, “Enhanced resilient state estimation using data-driven auxiliary models,” *IEEE Transactions on Industrial Informatics*, vol. 16, no. 1, pp. 639–647, 2020.
- [22] L. Wang and Q. Zhou, “Physics-guided deep learning for time-series state estimation against false data injection attacks,” in *2019 North American Power Symposium (NAPS)*. IEEE, 2019, pp. 1–6.
- [23] M. Huang, Z. Wei, G. Sun, and H. Zang, “Hybrid state estimation for distribution systems with ami and scada measurements,” *IEEE Access*, vol. 7, pp. 120 350–120 359, 2019.
- [24] C. Konstantinou and M. Maniatakos, “A case study on implementing false data injection attacks against nonlinear state estimation,” in *Proceedings of the 2nd ACM workshop on cyber-physical systems security and privacy*, 2016, pp. 81–92.
- [25] S.-E. Chien *et al.*, “Automation of contingency analysis for special protection systems in taiwan power system,” in *2007 International Conference on Intelligent Systems Applications to Power Systems*. IEEE, 2007, pp. 1–6.
- [26] X. Liu, J. Ospina, and C. Konstantinou, “Deep reinforcement learning for cybersecurity assessment of wind integrated power systems,” *IEEE Access*, vol. 8, pp. 208 378–208 394, 2020.
- [27] N. Mazzi, B. Zhang, and D. S. Kirschen, “An online optimization algorithm for alleviating contingencies in transmission networks,” *IEEE Transactions on Power Systems*, vol. 33, no. 5, pp. 5572–5582, 2018.
- [28] X. Liu and C. Konstantinou, “Reinforcement learning for cyber-physical security assessment of power systems,” in *2019 IEEE Milan PowerTech*. IEEE, 2019, pp. 1–6.
- [29] A. Keliris *et al.*, “Open source intelligence for energy sector cyberattacks,” in *Critical Infrastructure Security and Resilience*. Springer, 2019, pp. 261–281.
- [30] J. Kim, L. Tong, and R. J. Thomas, “Subspace methods for data attack on state estimation: A data driven approach,” *IEEE Transactions on Signal Processing*, vol. 63, no. 5, pp. 1102–1114, 2014.
- [31] D. P. Kingma and J. Ba, “Adam: A method for stochastic optimization,” *arXiv preprint arXiv:1412.6980*, 2014.
- [32] P. Venkatesh, R. Gnanadass, and N. P. Padhy, “Comparison and application of evolutionary programming techniques to combined economic emission dispatch with line flow constraints,” *IEEE Transactions on Power systems*, vol. 18, no. 2, pp. 688–697, 2003.
- [33] H. Mosbah and M. El-Hawary, “Multilayer artificial neural networks for real time power system state estimation,” in *2015 IEEE Electrical Power and Energy Conference (EPEC)*. IEEE, 2015, pp. 344–351.
- [34] B. Liu *et al.*, “Recognition and vulnerability analysis of key nodes in power grid based on complex network centrality,” *IEEE Transactions on Circuits and Systems II: Express Briefs*, vol. 65, no. 3, pp. 346–350, 2017.
- [35] J. Zhao *et al.*, “Power system dynamic state estimation: Motivations, definitions, methodologies, and future work,” *IEEE Transactions on Power Systems*, vol. 34, no. 4, pp. 3188–3198, 2019.